

# Surface Coordination Chemistry of Metal Nanomaterials

Pengxin Liu, Ruixuan Qin, Gang Fu,\* and Nanfeng Zheng\*<sup>ⓑ</sup>

State Key Laboratory for Physical Chemistry of Solid Surfaces, Collaborative Innovation Center of Chemistry for Energy Materials, Engineering Research Center for Nano-Preparation Technology of Fujian Province, and National Engineering Laboratory for Green Chemical Productions of Alcohols-Ethers-Esters, College of Chemistry and Chemical Engineering, Xiamen University, Xiamen 361005, China

**ABSTRACT:** Surface coordination chemistry of nanomaterials deals with the chemistry on how ligands are coordinated on their surface metal atoms and influence their properties at the molecular level. This Perspective demonstrates that there is a strong link between surface coordination chemistry and the shape-controlled synthesis, and many intriguing surface properties of metal nanomaterials. While small adsorbates introduced in the synthesis can control the shapes of metal nanocrystals by minimizing their surface energy via preferential coordination on specific facets, surface ligands properly coordinated on metal nanoparticles readily promote their catalysis via steric interactions and electronic modifications. The difficulty in the research of surface coordination chemistry of nanomaterials mainly lies in the lack of effective tools to characterize their molecular surface coordination structures. Also highlighted are several model material systems that facilitate the characterizations of surface coordination structures, including ultrathin nanostructures, atomically precise metal nanoclusters, and atomically dispersed metal catalysts. With the understanding of surface coordination chemistry, the molecular mechanisms behind various important effects (e.g., promotional effect of surface ligands on catalysis, support effect in supported metal nanocatalysts) of metal nanomaterials are disclosed.

## INTRODUCTION

The past decades have witnessed the rapid development of nanoscience and nanotechnology, especially in chemistry, physics and materials science.<sup>1–3</sup> Size and surface characteristics are the two commonly recognized factors for many so-called “nano-effects” leading to unique physical and chemical properties of nanomaterials.<sup>3</sup> Take semiconducting quantum dots as an example. Although size is the major determinant to their tunable electronic and optical properties,<sup>4</sup> recently increasing studies have demonstrated that the coordination chemistry of surface ligands on quantum dots is crucial as well to their photoluminescence quantum yield and even processability.<sup>5–7</sup> The importance of surface coordination chemistry of nanomaterials has been attracting increasing attention in nanoscience and nanotechnology.<sup>8</sup> Metal nanomaterials represent another research focus in the area of nanomaterials owing to their fascinating properties and thus promising applications in optics, electronics, catalysis and so on.<sup>9,10</sup> Surface plasmon resonance (SPR) is one of the most interesting phenomena of nanoscale metallic particles. SPR is

the collective property of metal nanoparticles and highly dependent on their overall morphologies. How to control the shape of metal nanoparticles is thus the key to tailor their optical properties. Although the coordination chemistry on metal nanoparticles occurs at the much smaller size scale from that to manipulate their SPR, the past decade has seen the important role of small ligands in controlling the shape of metal nanoparticles and thus their SPR properties.<sup>9–11</sup>

The shape of metal nanoparticles influences not only their SPR properties but also their catalytic performances.<sup>12–14</sup> As a surface-controlled process, heterogeneous catalysis is closely connected to the detailed surface structure of catalysts. In heterogeneous catalysis involving metal centers, the reactants are typically activated by diffusing onto the catalyst surface and forming chemical bonds via surface coordination. Surface metal atoms on different facets of a solid are usually in different coordination environments, therefore offering different activation capabilities to reactants. This is the major principle behind the surface-dependent catalysis, and might explain why so many effects (e.g., size, shape, support, alloy) are associated with heterogeneous catalysts based on metal nanoparticles.

As shown in Figure 1, at the molecular level, various metal coordination sites (terrace, edge, kink, or corner sites) are present on a fine metal nanoparticle. These sites could exhibit quite different coordination chemistry toward reactants, intermediates and products.<sup>15</sup> And the distribution of these

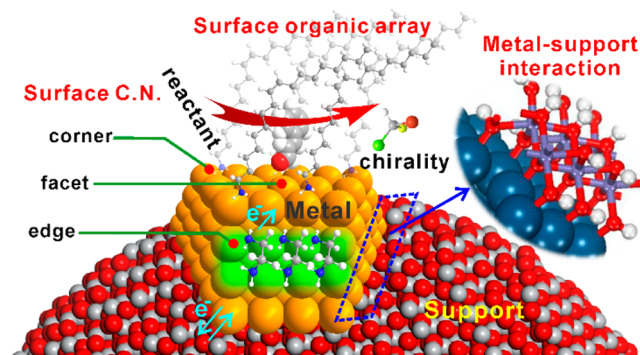


**Figure 1.** Involvements of coordination chemistry on the surface and interface of metal nanomaterials in different aspects: coordination number (C.N.) of surface metal atoms; coordinating ligand array interfering the reactants' interaction with metal; electronic effect induced by surface coordinating ligands; the local coordination environments of metal–support interface.

Received: October 20, 2016

Published: January 13, 2017

sites is often dependent on the size or shape of metal nanoparticles, inducing many size- and shape-effects. Moreover, in catalysis, metal nanoparticles are often supported on high-surface area materials to prevent their aggregation.<sup>2</sup> Loading metal nanoparticles on supports can significantly alter the coordination environment of metal atoms in the contacting area, introducing many support-effects in heterogeneous catalysis. However, understanding the molecular mechanisms behind those intriguing effects and therefore better controlling the heterogeneous catalysis is still of great challenge.

As for industrial applications, the increasing environment concerns and the climbing costs of waste disposal have been reinforcing the development of heterogeneous catalysts having both high activity and selectivity.<sup>16–18</sup> In numerous chemical processes involving the use of metal nanocatalysts, additives are frequently used to improve the selectivity toward desired products. Many those additives are good ligands to coordinatively modify the catalytic surface for promoting selectivity.<sup>19–23</sup> The perfect design of surface modifiers relies on the deep understanding on the surface coordination chemistry of metal catalysts. Although surface coordination is so important to explain the nature behind “nano-effects” (e.g., particle size, shape, support) in nanocatalysis, the lack of effective tools to characterize the detailed surface and interface structures of metal nanoparticles has largely prevented us from deeply understanding the surface coordination chemistry on metal nanomaterials.

In this Perspective, we will focus on the practice of surface coordination chemistry to tailor the morphology and catalytic properties of metal nanocrystals at the molecular level. We will first discuss how the surface coordination of small ligands influences the surface structure and morphology of metal nanocrystals, and thus their properties. The significant impacts of surface ligands on the catalytic properties of metal nanocrystals will also be demonstrated. Two important effects (steric and electronic effects) will be discussed on how surface coordination chemistry controls in particular the catalytic selectivity. The much difficulty to understand the role of surface ligands on catalysis lies in the lack of effective techniques to resolve the interfacial structure of ligands on metal surfaces at the molecular level. Following the discussion on the effects of surface ligands on catalysis, ligand-protected atomically precise metal nanoclusters will be proposed as a model system for “seeing” how surface ligands are surface-coordinated on metal nanoparticles. Together with some breakthroughs in resolving total structures of metal nanoparticles, examples on using atomically precise metal nanoclusters to demonstrate the promoting effect of surface ligands on catalysis will be given. The concept of surface coordination chemistry will be extended to catalysts based on supported metal nanoparticles by discussing how the coordination environment surrounding the catalytic metal sites determines the activity and selectivity of supported metal nanocatalysts.

## ■ SURFACE COORDINATION IN THE SHAPE-CONTROLLED SYNTHESIS OF METAL NANOCRYSTALS

During the past decades, the shape-controlled synthesis of metal nanocrystals has attracted increasing research interests owing to their unique shape-dependent optical properties and surface reactivity.<sup>9,10</sup> Noble metals are typical of face-centered cubic (fcc) structure. To minimize their surface energies, noble metal nanocrystals would thermodynamically prefer to grow

into cubooctahedrons (near spheres) enclosed by {111} and {100} facets due to the Wulff construction. The formation of noble metal nanocrystals of anisotropic shapes requires the delicate control over the growth thermodynamics and kinetics in the synthesis.

Several recent reviews have nicely summarized the keys in the shape-controlled synthesis of metal nanocrystals.<sup>9–11,24–26</sup> In this Perspective, we only emphasize how the surface coordination of small ligands facilitates the shape-controlled synthesis of metal nanocrystals. As shown in Figure 2, the

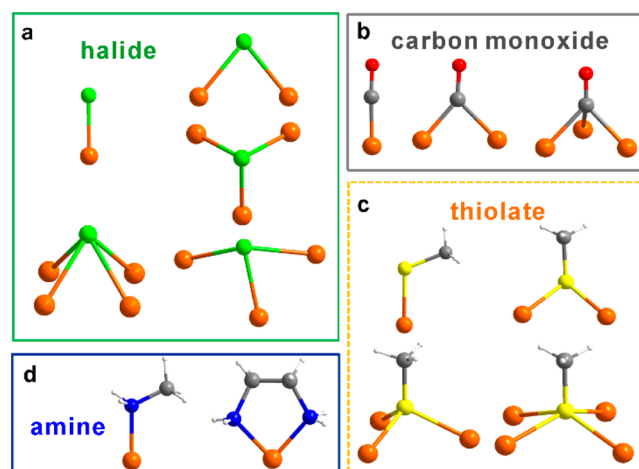


**Figure 2.** Typical coordination structures of small ligands: (a) halide, (b) carbon monoxide, (c) thiolate, (d) amine. Color codes: Orange, metal atoms; green, halide; gray, C; red, O; blue, N; yellow, S; white, H.

coordination structures vary with types of ligands. The strong surface coordination of small adsorbates would significantly reduce the surface energies of facets that they preferentially bind, thus leading to the formation of nanocrystals with non-Wulff shapes. For instance, halides coordinate strongly to metals with different binding modes (Figure 2a). The presence of halides, commonly found in metal precursors (e.g.,  $\text{AuCl}_4^-$ ,  $\text{PdCl}_4^{2-}$ ) and capping agents such as cetyltrimethylammonium bromide, has been well-documented in the community to be an important factor to control the shape of Au nanocrystals.<sup>26,27</sup> Similarly, Pd nanocubes/nanowires and Rh nanocubes were prepared due to the selective binding of halides on Pd/Rh{100}.<sup>28–31</sup> The strong coordination binding of halide on Pd{100} has been well-investigated in the field of surface science.<sup>32</sup>

Due to its strong coordination strength and also rich binding modes (Figure 2b), CO has been emerging as an effective small ligand in the shape-controlled synthesis of metal nanocrystals.<sup>11,33</sup> Many transition metals form carbonyl coordination complexes. The chemisorption of CO on metal surfaces has inspired numerous experimental and theoretical studies. The binding structures of CO on metal surface are mainly in three different modes (i.e., atop, bridge, and hollow) (Figure 2b) which are readily identified by infrared spectroscopy.<sup>34</sup> The variation in the electronic structure and atomic radii of metals often makes CO coordinate on their surfaces in different modes. For example, we have found that CO prefers to coordinate on Pd {111} facets in bridge and hollow modes.<sup>35</sup> Such a preferential surface coordination of CO on Pd allows the confinement growth of freestanding ultrathin plasmonic Pd

nanosheets (Figure 3a).<sup>33</sup> By simply introducing CO as reducing agent and surface confining agent, ultrathin Pd

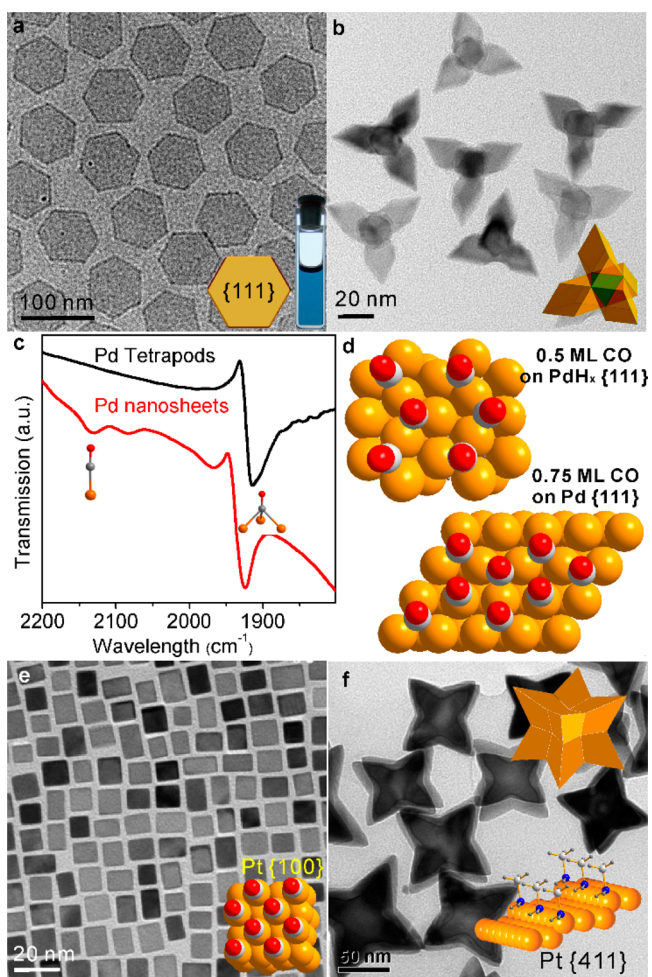


**Figure 3.** Surface coordination of small ligands facilitates the shape-controlled synthesis of metal nanocrystals. (a) Ultrathin hexagonal Pd nanosheets by CO and halide; (b) Pd tetrapods by the use of CO and H<sub>2</sub>; (c) FTIR spectra and (d) the proposed binding structures of CO on Pd nanosheets and tetrapods; (e) Pt nanocubes made by the linear adsorption of CO; (f) Amine-assisted formation of Pt octapods enclosed by high-index {411} facets. Panel (a) is reproduced from ref 33. Copyright, Nature Publishing Group 2011. Panel (b–d) and (f) are reproduced with permission from refs 45 and 55, respectively. Copyright, American Chemical Society 2012 and 2011. Panel (e) is reproduced from ref 47. Copyright, the Royal Society of Chemistry 2011.

nanosheets having {111} facets as their major exposure surface and a thickness of several atomic layers (~1.8 nm) were easily obtained. When halides (e.g., Br<sup>-</sup> and Cl<sup>-</sup>) were introduced into the synthesis together with CO, the ultrathin Pd nanosheets showed hexagonal shape due to the selective binding of halides on the side Pd {100} facets. Unfortunately, such a critical role of CO in the formation of ultrathin Pd nanosheets was not recognized in the early work.<sup>36,37</sup>

Since the copresence of CO and halide was the key factor for the formation of hexagonal Pd nanosheets, their synthesis was further simplified by mixing H<sub>2</sub>O with [Pd<sub>2</sub>(μ-CO)<sub>2</sub>Cl<sub>4</sub>]<sup>2-</sup> in DMF at room temperature.<sup>38,39</sup> When reacted with H<sub>2</sub>O, part of the coordinating CO on [Pd<sub>2</sub>(μ-CO)<sub>2</sub>Cl<sub>4</sub>]<sup>2-</sup> was oxidized to CO<sub>2</sub>. Consequently, two electrons from each oxidized CO

reduced the two Pd(I) into Pd(0), leading to the formation of ultrathin Pd nanosheets. The ultrathin Pd nanosheets were blue in color and exhibited a well-defined SPR peak with strong absorption in the near-infrared region (NIR). Together with their high NIR photothermal effect, the excellent photothermal stability makes these Pd nanosheets a promising agent for NIR cancer photothermal therapy.<sup>33</sup> More importantly, the understanding over the formation mechanism of Pd nanosheets allows us to systematically prepare different-sized Pd nanosheets.<sup>40–42</sup> Such a capability provides an excellent material platform for investigating the size-effect in the biobehaviors of 2D nanosheets, which has not yet been achieved in other 2D materials.

It should be noted that the formation of Pd nanosheets assisted by CO or carbonyl compounds was also observed by other groups.<sup>43,44</sup> Ultrathin Pd nanosheets are not expected as a thermodynamically stable nanostructure. These nanosheets were yielded mainly because of the “poisoning” effect of high coverage of CO that prevents the continuous deposition of Pd(0) atoms on Pd{111}. When CO and H<sub>2</sub> were simultaneously used to reduce Pd(acac)<sub>2</sub>, observed was the formation of single-crystalline Pd tetrapods and tetrahedra enclosed by {111} facets (Figure 3b).<sup>45</sup> The formation of β-PdH<sub>x</sub> reduced the CO binding energy on Pd and thus helped to decrease the CO coverage, which was the key for the formation of Pd tetrapods and tetrahedra. The mechanism was confirmed by FTIR and DFT studies (Figure 3c, 3d).

Ultrathin Rh nanosheets with Rh{111} basal planes were also prepared when CO was introduced in the synthesis.<sup>46</sup> The similar role of CO on the synthesis of Pd and Rh nanosheets is attributed to the similar coordination of CO on their {111} facets. However, the surface coordination chemistry of CO on Pt is quite different from that on Pd. CO prefers to linearly coordinate on Pt{100}. Hence, the involvement of CO in the synthesis of Pt nanocrystals often led to the formation of Pt nanocubes enclosed by Pt{100}.<sup>47,48</sup> Although early studies revealed that introducing metal carbonyls [e.g., Fe(CO)<sub>5</sub>, Co<sub>2</sub>(CO)<sub>8</sub>, W(CO)<sub>6</sub>] facilitated the formation of nanocubes of Pt and their alloys,<sup>49–51</sup> the role of CO was ignored. Later reports revealed that the use of CO was capable to induce the formation of Pt nanocubes (Figure 3e).<sup>47,48,52</sup> The preferential linear coordination of CO on Pt{100} was then demonstrated as the main reason why Pt nanocubes were yielded in the synthesis involving the use of CO. It should be noted the CO-assisted strategy also worked in the synthesis of Pt-based alloy nanocrystals enclosed by {100} facets.<sup>53</sup>

In addition to CO and halides, many other small adsorbates that can control the surface structures and morphologies of metal nanocrystals have been demonstrated.<sup>9,11,24</sup> For instance, Yang et al. demonstrated that increased ratio of NO<sub>2</sub> to Pd helps to synthesize nanocrystals with more Pd{111} facets exposed, on account of the stabilization effect of NO<sub>2</sub> on Pd{111}.<sup>54</sup> High-index facets of fcc metals are enriched of low-coordinated metal sites and often exhibit excellent catalytic performances. The coordination binding of amines on low-coordinated metal sites stabilizes high-index facets, providing an effective strategy to prepare Pt-based nanocrystals enclosed by high-index facets (Figure 3f).<sup>55</sup>

## ■ SURFACE COORDINATION PROMOTES CATALYSIS

In homogeneous catalysis and biocatalysis, catalytically active metal centers are coordinated with ligands and biomolecules. The ligands create a delicate local environment to induce

significant steric and electronic effects that tailor the overall catalysis, especially selectivity.<sup>21,56,57</sup> Polymeric or small organic ligands are often used in the synthesis of high-quality metal nanocrystals to prevent their aggregation or control their shapes. However, two opposite effects of surface ligands on catalysis have been reported in the literature.<sup>18,58</sup> The presence of surface agents has been long considered to block the surface active sites of metal nanocrystals and thus be deleterious to their catalytic activities. Surface ligands are thus often removed by post-treatments to optimize their catalytic activities.<sup>22</sup> However, during the past decade, an increasing number of studies demonstrate the promoting effects of surface ligands on the catalysis of metal nanocrystals, particularly their selectivity. For instance, in the industrial Lindlar catalysts,<sup>19</sup> together with toxic metals such as lead, other “poisons” (e.g., quinoline, sulfide) are used to improve the selectivity of Pd nanocatalysts toward the semihydrogenation of alkynes to alkenes. The two-face effects of surface ligands on catalysis of metal nanoparticles are highly related to their surface coordination chemistry.

In order to make positive effects on catalysis, the surface ligands coordinating on metal nanocrystals should at least meet the following two conditions: (1) The coverage of surface ligands on nanocrystals should not be too high to block all the surface active sites; (2) The ligands must alter the interaction between reactants/intermediates and catalyst surface. As for the coverage, different types of ligands bind on metal surface in different coordination structures. For example, similar to the situation of CO, thiol ligands bind strongly to surface metal atoms in rich coordination configurations (Figure 2c).<sup>59</sup> The rich coordination chemistry of thiols makes them easily spread out over metal surfaces and thus drastically poison their catalytic sites. In contrast, the coordination chemistry of alkylamines is rather simple. They are bonded to surface metal atoms relatively weakly. When coordinated to metal atoms, amines mainly serve as one-coordinated ligands (Figure 2d). Together with such a coordination feature of amines, the van der Waals interaction among organic groups on amines helps to limit their surface coverage on metal nanocrystals and leave some surface metal atoms accessible for small reactants. It is thus not surprising that many amine-capped metal nanocrystals still exhibit excellent catalysis toward various reactions.<sup>58,60</sup>

When the surface atoms are not fully covered, the surrounding ligands should influence the catalysis of nearby catalytic metal sites via steric and electronic effects. A nice example of the steric effect is to use bulky chiral ligands to modify the surface of metal nanocatalysts to create heterogeneous catalysts for enantioselective hydrogenation.<sup>61–63</sup> For example, Pt nanocatalysts surface-modified with cinchona alkaloids have been used as effective catalysts for the enantioselective hydrogenation of ketones (Figure 4a).<sup>63</sup> Using organic modifiers to manipulate the interaction structure between reactants and catalytic surface has been recently extended far beyond for enantioselective hydrogenation. Organically modified heterogeneous metal catalysts are also widely investigated in chemoselective hydrogenation which involves multiple hydrogenation sites or steps.<sup>60,64–66</sup> For instance, the deposition of *n*-alkanethiol self-assembled monolayers onto the surface of Pd nanoparticles enhanced catalytic selectivity in 1-epoxy-3-butene (EpB) hydrogenation (Figure 4b).<sup>64</sup> In comparison with uncoated palladium catalysts that showed selectivity to epoxybutane at 313 K of 11%, thiols modified Pd catalysts greatly improved selectivity up to 94% at the same EpB conversion.

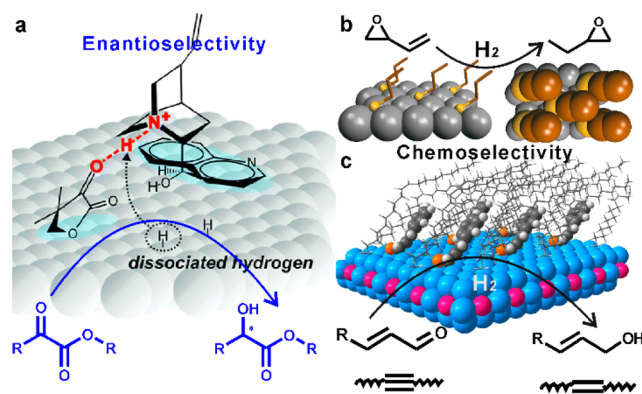


**Figure 4.** Surface coordination creates steric effects to promote catalytic selectivities in hydrogenation reactions. (a) Surface modification with cinchona alkaloids on Pt improves enantioselectivity. (b) Surface adsorption of thiols on Pd enhances the hydrogenation of 1-epoxy-3-butene to 1-epoxy-3-butane. (c) The presence of surface oleylamine array makes metal nanocrystals as highly selective catalysts for the hydrogenation of C=O and C≡C bonds. Panel (a) and (c) are reproduced from ref 63 and 60, respectively. Copyright, Wiley 2014 and 2010. (b) is reproduced with permission from ref 64. Copyright, Nature Publishing Group 2010.

Enzymes can enhance the biological reactions with ultrahigh specificity by means of forming hydrogen bonds between the substrates and the surrounding amino acid groups. The surface ligands on nanomaterials can also sometime improve the chemoselectivity in the similar way. Recently, Kunz and co-workers prepared Pt nanoparticles by a colloidal approach and modified their surface with *L*-proline before supporting them on Al<sub>2</sub>O<sub>3</sub>.<sup>67</sup> As compared with unmodified Pt nanoparticles, modified Pt nanoparticles exhibits extremely high chemoselectivity in the hydrogenation of acetophenone toward phenylethanol with a modest stereoselectivity, 14% enantiomeric excess (ee), at 100% conversion. More impressively, a dual effect of *L*-proline was observed with the high chemoselectivity accompanied by an enhanced rate toward the desired product. While the enhanced chemoselectivity was attributed to the high coverage of proline that helps to dilute Pt ensembles and thus inhibit undesired reactions of the phenyl group, the promoted activity was attributed to N–H on the ligand.

Despite post-treatments to introduce surface modifiers for enhancing catalysis of metal nanocatalysts, surface capping agents, such as oleylamine (OAm), widely used in the synthesis of high-quality nanocrystals are barely considered as promoters for selective catalysis. These agents were usually removed before catalysis. However, we recently showed that OAm on Pt<sub>3</sub>Co nanocrystals promoted the chemoselectivity in the hydrogenation of cinnamyl aldehyde (CAL) (Figure 4c).<sup>60</sup> DFT calculations revealed that OAm ligands formed an ordered coordination array on nanocrystals so that CAL molecules had to insert into the amine forest with only their terminal C=O bonds reacting with the catalytic surface. Such an interaction structure prevented the C=C bond activation, leading to >90% selectivity toward C=O hydrogenation. When OAm was replaced by shorter-chain amines, the weaker van der Waals interactions among ligands destroyed the ordered array. CAL would then lay down on metal surface, resulting in poor selectivity toward C=O hydrogenation. Interestingly, alkyl-amine-capped Pt<sub>3</sub>Co also displayed a selectivity of over 90% to semihydrogenated alkenes at the full conversion of alkynes.<sup>68</sup>

In addition to steric effect, electronic effect is another important factor to manipulate the selectivity in catalysis. Coordination bonds are formed by donating electrons from ligands (Lewis bases) to metal centers (Lewis acids). Coordination of ligands should thus alter the electronic structure of metals. Such an electronic modification is expected to make an impact on catalysis of metal catalysts. Although the electronic effect of ligands has been widely applied to optimize homogeneous catalysis by metal complexes, it has been much less recognized in the field of heterogeneous catalysis. In literature, there have been rare reports proposing the electronic effect of organic modifiers on the catalysis of metal nanocatalysts.<sup>69,70</sup> Such a situation is mainly caused by the following two situations: (1) Heterogeneous metal catalysts are in general highly complicated materials. Currently, there is lack of effective tools to characterize the metal–ligand interfaces within those catalysts; (2) To maximize their effects on catalysis, electrons donated from ligands should localize on the surface of metal components. How to probe the surface electronic structures is another challenging issue.

Recently, our group has successfully prepared ethylenediamine (EDA)-coated ultrathin Pt nanowires (EDA-Pt NWs) as a model catalyst to demonstrate that surface organic modifiers on heterogeneous metal catalysts readily induce a perfect interfacial electronic effect to shape their catalytic selectivity (Figure 5).<sup>23</sup> The ultrathin Pt nanowires having only EDA on

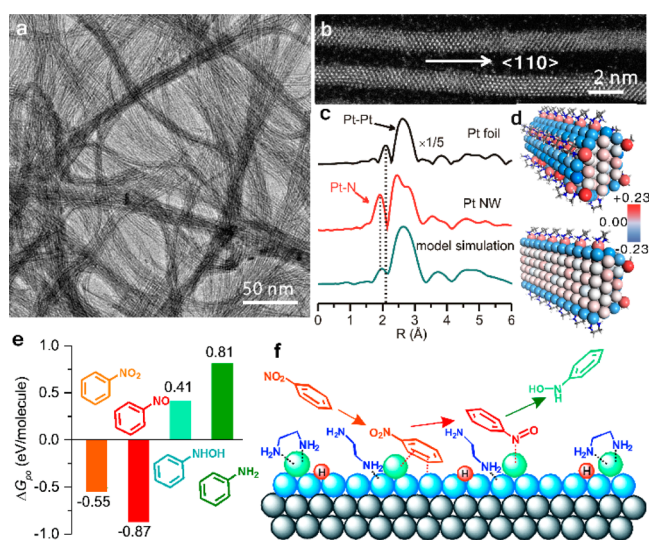


**Figure 5.** Electronic effect of surface coordination in promoting catalytic selectivity demonstrated by EDA-chelated ultrathin Pt nanowires. (a) TEM image, (b) high-resolution TEM image and (c) EXAFS spectra of EDA-Pt NWs; (d) The Bader charge analysis of EDA-Pt NWs; (e) Free energies for the adsorption of N-containing aromatics over EDA-Pt NWs; (f) Scheme showing the mechanism on how interfacial electronic effect improves catalytic selectivity to *N*-hydroxylaniline. Reproduced with permission from ref 23. Copyright, Nature Publishing Group 2016.

their surface were prepared by chemically reducing Pt(acac)<sub>2</sub> in the presence of EDA but the absence of any polymeric capping agent. The ultrathin feature of the nanowires makes it possible to fully characterize the metal–ligand interfacial structure using X-ray absorption spectroscopy, which is very important to deeply understand the effect of surface ligands on catalysis. In the hydrogenation of nitrobenzene at room temperature, the catalyst exhibited an unexpectedly high selectivity for the

production of *N*-hydroxylanilines, a thermodynamically unfavorable but industrially important compound. Over the ultrathin EDA-Pt NWs, the selectivity for *N*-hydroxylaniline was nearly 100% at the full conversion of nitrobenzene at 50 min, and well maintained even when the reaction time was prolonged to 2 h. Such a high selectivity cannot be achieved by pristine Pt nanocatalysts.

DFT calculations revealed that the electron donation from EDA made the surface of Pt NWs highly electron rich, thus favoring the adsorption of electron-deficient reactants over electron-rich substrates (*N*-hydroxylanilines) and preventing its full hydrogenation into anilines. The electron-rich surface was also expected to enhance CO binding by back-donating more electrons into CO, confirmed by the CO stripping higher oxidative stripping potential than that on Pt blacks. With the understanding of how chelating EDA on Pt NWs improved the catalytic selectivity, Pt black was treated to allow the deposition of Pt-EDA chelating units on its surface to alter their surface electronic structure. As expected, the modified Pt black catalyst exhibited a high selectivity to *N*-hydroxylaniline (>97%). The concept by using interfacial electronic effect to improve catalytic selectivity also worked for the nitroaromatics with different substitutions.

Although the surface coordination of organic ligands creates both steric and electronic effects for promoting the catalytic properties of metal nanoparticles, it is particularly important for practical applications that the coordination of surface organic modifiers on metal nanoparticles is strong enough to prevent them from being deattached during catalysis. The use of surface modifiers bearing strong coordination sites or even chelating groups (e.g., thiolates, diamines) is thus preferred. The introduction of excess surface modifiers to the catalytic reactions helps to make up the ligand desorption from metal surface, providing an effective alternative to stabilize catalytic performances of organic-modified metal nanocatalysts for practical applications.

Most heterogeneous catalysts were complex with many factors affecting the catalytic properties, including composition, size, shape, and surface structure of metal nanoparticles. As discussed above, in the case of ultrathin Pt NWs, the interesting interfacial electronic effect was discovered and well-understood mainly because of the well-defined ultrathin structure of the Pt NWs that allows the full characterizations of their detailed surface and interface structures. Although the conclusion was straightforward, much effort has to make on the synthesis of ultrathin nanostructures and their structural characterizations due to the lack of good tools to “see” the surface ligands on metal nanoparticles.

## ■ ATOMICALLY PRECISE METAL NANOCCLUSERS AS MODEL SYSTEMS FOR STUDYING SURFACE COORDINATION

The structures of metal nanomaterials are typically characterized by electron microscopy which is however not powerful enough to resolve their detailed surface coordination structures. Due to their molecular monodispersity, organic-stabilized atomically precise metal nanoclusters are readily crystallized into long-ordered single crystals, allowing the use of X-ray single crystal analysis to characterize their total structures at the molecular level.<sup>71,72</sup> Atomically precise metal nanoclusters can thus serve as an extremely ideal system to study the coordination chemistry on metal nanoparticles. For instance,

the structure resolution of  $\text{Au}_{102}(\text{SR})_{44}$  nanoparticles in 2007 has made a significant impact on the field of monolayer-protected metal nanoparticles (Figure 6a).<sup>73</sup> Since then, the

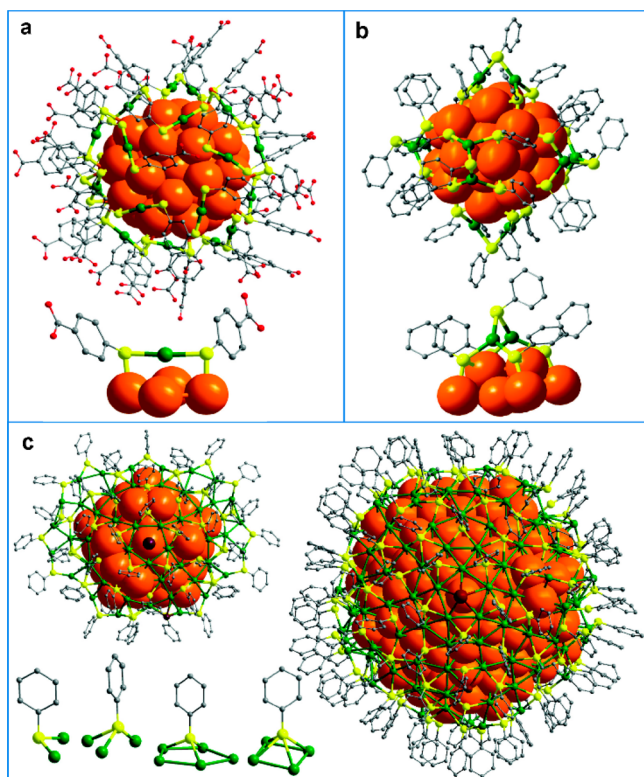


**Figure 6.** Total structures of organic-capped metal nanoclusters resolved by X-ray diffraction techniques: (a)  $\text{Au}_{102}(\text{SR})_{44}$ ; (b)  $[\text{Ag}_{44}(\text{SR})_{30}]^{4-}$ ; (c)  $\text{Ag}_{136}$  and  $\text{Ag}_{374}$ . Their surface coordination motifs are highlighted as insets. Color Codes: Orange/green, metal; yellow, S; gray, C; red, O; brown, halide. The figures are reproduced from the cif files reported in refs 73, 78 and 80.

presence of  $-\text{RS}-\text{Au}-\text{SR}-$  staple units has been widely accepted as a common surface structure motif of thiol-stabilized Au nanoparticles, changing our previous visions on their surface structures.<sup>74–76</sup> Such a finding has been recognized as a breakthrough and widely applied as a surface structure model for thiolated Au nanoparticles and even thiol self-assembly monolayer on Au.<sup>77</sup>

In the community of metal nanoparticles, it has been long proposed that thiols on Ag nanoparticles should have the similar surface structure to that on Au nanoparticles. However, in 2013, the structure resolution of  $[\text{Ag}_{44}(\text{SR})_{30}]^{4-}$  clusters revealed that the coordination structure of surface thiolates on Ag nanoparticles was much more complicated than that on Au nanoparticles (Figure 6b).<sup>78,79</sup> More recently, the total structures of two giant thiolated Ag nanoparticles containing 136 and 374 Ag atoms were also successfully characterized by single-crystal X-ray analysis (Figure 6c).<sup>80</sup> As the largest thiolated metal nanoparticles crystallographically determined so far, these Ag nanoparticles are miniatures of two 5-fold twinned Ag nanostructures (i.e., decahedral nanoparticles and twinned nanorods). Structurally, a decahedral nanoparticle is bound by ten (111) facets and a 5-fold twinned nanorod/nanowire of fcc metals is enclosed by five (100) facets at its side and ten (111) faces at two ends. However, the outermost Ag atoms, particularly on (111) facets of thiolated  $\text{Ag}_{136}$  and  $\text{Ag}_{374}$

nanoparticles did not adopt the close-packed arrangement at all, strongly suggesting the significant impact of surface coordination of thiolate on the surface structure of Ag nanoparticles. Such detailed structure information cannot be simply observed by electroscopic techniques. Similarly, very recently, the cause of phosphine and thiolate ligands was demonstrated to be critical for the formation of serial Ag cubes.<sup>81</sup>

Another important feature of atomically precise metal nanoclusters is that their optical absorption properties are highly sensitive to their metal-framework structures. UV–vis spectroscopy is effective to evaluate the structural change after removing their surface ligands through thermal treatment for example. The clusters whose surface ligands are removable while keeping their metal framework structures intact are ideal systems for investigating the influence of surface ligands on catalysis of metal nanoparticles.<sup>82,83</sup> An intermetallic nanocluster,  $\text{Au}_{34}\text{Ag}_{28}(\text{PhC}\equiv\text{C})_{34}$  was recently used as such a model catalyst to explore the importance of surface ligands in promoting catalysis (Figure 7).<sup>83</sup> All phenylalkynyl (PA)

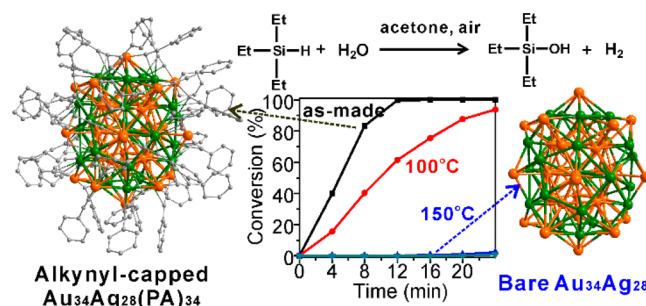


**Figure 7.** Surface coordination on  $\text{Au}_{34}\text{Ag}_{28}(\text{PhC}\equiv\text{C})_{34}$  nanoclusters promotes their catalysis in the hydrolytic oxidation of organosilanes. Reproduced from ref 82. Copyright, American Chemical Society 2016.

ligands are linearly coordinated to surface Au atoms with staple “ $\text{PhC}\equiv\text{C}-\text{Au}-\text{C}\equiv\text{CPh}$ ” motif and can be removed at relatively low temperatures. The UV–vis spectrum of the cluster treated at 150 °C showed almost the same, suggesting that its metal framework remained intact after the treatment. It is impressive that the parental cluster showed high catalytic activity in the hydrolytic oxidation of organosilanes to silanols. The turnover frequency was as high as  $116\,000\text{ h}^{-1}$  for each surface Au atom, over 3 times higher than the highest number reported.<sup>84</sup> However, after treatment at 150 or 200 °C to remove the surface PA ligands, the cluster displayed negligible catalytic activity. The organic-capped metal nanoclusters could work as active catalysts much better than those with surface ligands partially or completely removed, which might be explained by the synergetic activation of silanes and  $\text{H}_2\text{O}$  at the Au–PA interface.

## ■ COORDINATION CHEMISTRY AT THE INTERFACE OF SUPPORTED METAL CATALYSTS

Although supported catalysts are the most widely used catalysts in industry, the fundamental understanding of their catalysis remains challenging. Many factors are implicated in shaping the performances of supported catalysts. Supports often play critical roles in stabilizing and promoting the catalysis of supported metal nanoparticles.<sup>85–88</sup> The concept of “support effects” has been brought for long, but the chemistry behind them remains blurring. Supported catalysts prepared by conventional methods carry various metal species, which can be single

ions, nanoparticles of various sizes and interfacial sites.<sup>89</sup> It is unpractical to simply correlate their catalytic performances with the observed macroscopic support effects. However, currently few characterization techniques are powerful enough for investigations down to subnanometer where chemistry actually takes place. Therefore, the design of model catalysts that facilitate the characterization of real active sites is highly desirable.

A desirable model nanocatalyst for investigating the chemistry at the interface between metal and support components should have uniform catalytically active sites and ideally minimize either metal or support components only at the interface at the atomic scale. As shown in Figure 8, the

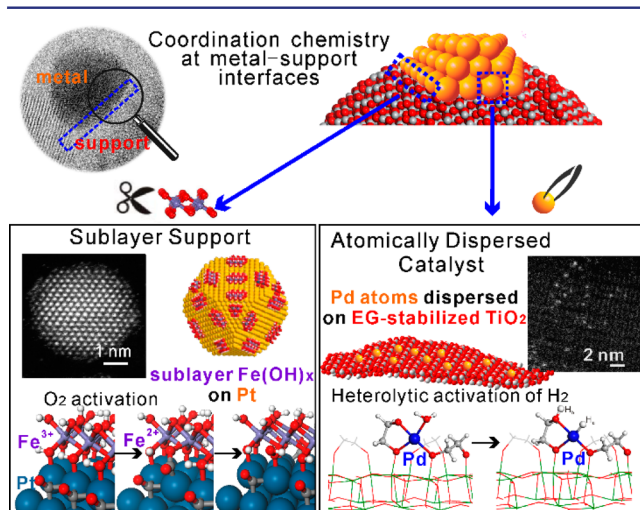


**Figure 8.** Two structural strategies to create model nanocatalysts for understanding the coordination chemistry at the interfaces of supported metal nanocatalysts. Two examples of the inverse (left) and atomically dispersed (right) structures are given at the bottom. The bottom left and right panels are reproduced with permission from refs 92 and 96. Copyright, American Association for the Advancement of Science 2014 and 2016.

following two structural strategies are effective to create model catalysts to understand the interface chemistry of supported nanocatalysts: (1) An inverse structure with metal nanoparticles whose surfaces are partially covered by submonolayer support components;<sup>90–93</sup> (2) An atomically dispersed structure with metal components dispersed as single metal sites on supports.<sup>94–101</sup> In the reverse structure, all support components are minimized and located only at the interface, avoiding the interference of noninterface support components in the interface characterizations. In contrast, atomically dispersed catalysts minimize metal components into single metal atoms which are all located at the interface. The structure information obtained from these metal sites should reflect exactly the interface's local coordination environment.

The decades' development of wet-chemical strategies for the synthesis of nanomaterials with well-defined structure parameters has facilitated the preparation of model catalysts of two different structures discussed above.<sup>17,18,102</sup> For example, we have recently developed an effective wet-chemistry to deposit atomically thick metal hydroxide (M–OH) on the surface of monodisperse Pt nanocrystals.<sup>92</sup> The M–OH species function as ligands, forming abundant interfacial active sites M–OH–Pt, just like organic modifiers do. When submonolayer Fe–OH was deposited onto Pt, obtained was a model catalyst highly

active for CO oxidation at room-temperature. While X-ray absorption fine structure (XAFS) indicated a slightly distorted octahedral coordination of interfacial Fe<sup>3+</sup>, X-ray photoelectron spectroscopy (XPS) revealed that the ligands surrounding Fe<sup>3+</sup> were mainly OH<sup>–</sup>. With such structural information, both DFT calculations and isotope-labeling experiments strongly confirmed that the interfacial Fe<sup>3+</sup>–OH–Pt sites were the major active sites for room-temperature CO oxidation initiated by the oxidative coupling of coordinated CO on Pt and interfacial –OH. Such a mechanism nicely explains why FeO<sub>x</sub> is an excellent support for Pt catalysts in CO oxidation. Moreover, the inverse structure also helped to discover that the incorporation of regular six-coordinated Ni<sup>2+</sup> into the interfacial M–OH layers stabilized the M–OH–Pt from dehydration and thus losing the active sites. The Pt/FeNi(OH)<sub>x</sub> catalyst was stable in the reaction stream for more than 28 h without any significant decay at room temperature. More importantly, with this understanding, an alloy-assisted strategy was developed to produce a practical Pt nanocatalyst with maximized M–OH–Pt sites.

Atomically dispersed catalysts are another ideal system that allows the identification of local coordination environment of metal active sites by currently available techniques such as XAFS. In these model catalysts, one can consider the support as ligands by providing its binding sites for metal atoms. If every metal atom is in the same chemical environment, these atomically dispersed catalysts should behave as homogeneous catalysts while retaining heterogeneous catalysts' advantages, bridging the huge gap between these two catalyst systems. The big challenge in the preparation of atomically dispersed metal catalysts is to increase the loading of active metal components to make the catalysts effective enough for the structure characterization of active sites and also for practical applications.<sup>95</sup> During the past decade, significant progress has been made to increase the metal loading in atomically dispersed catalysts. For example, we have recently developed a photochemical strategy to prepare a highly stable atomically dispersed Pd catalyst (Pd<sub>1</sub>/TiO<sub>2</sub>) with Pd loading over 1.5 wt % on ultrathin ethylene glycolate (EG)-functionalized TiO<sub>2</sub> nanosheets.<sup>96</sup> The Pd centers in the catalyst are square-planarly coordinated by four oxygen atoms (two from EG fixed on Ti, one from unbound O on EG, and one from coordinated H<sub>2</sub>O). With the formation of such a unique Pd–EG–TiO<sub>2</sub> coordination interface, the Pd centers activated H<sub>2</sub> via heterolytic splitting. According to DFT calculations, H<sub>2</sub> adsorbed on Pd atom was readily split into two H atoms. One of the H atoms moved to nearby oxygen on EG to yield O–H<sup>δ+</sup>, leaving the other H atom on Pd as H<sup>δ–</sup>. In the hydrogenation of styrene over Pd<sub>1</sub>/TiO<sub>2</sub>, both H<sup>δ–</sup> and H<sup>δ+</sup> were involved, which was confirmed by both IR and NMR measurements performed with deuterium-labeled reagents. The catalyst was highly stable with no activity decrease after 20 cycles of reuse. It is interesting that heterolytic cleavage of H<sub>2</sub> has been usually observed over homogeneous catalysts (Au, Pd and Ru complexes), but rarely reported on heterogeneous Pd catalysts. Due to the unique activation mechanism, Pd<sub>1</sub>/TiO<sub>2</sub>-EG system showed high catalytic activity in the hydrogenation of aldehyde at room temperature with a turnover frequency (TOF) of >55 times higher than that of surface Pd atoms on commercial Pd catalysts. The coordination bonds between EG and Pd atoms not only stabilize single Pd atoms, but also play an important role in catalysis. As expected, the atomically dispersed catalysts

serve as a nice bridge between homogeneous catalysts and heterogeneous catalysts.

In order to capture the local coordination environment of catalytically active sites, the central idea is the same in the both cases discussed above. By minimizing the support to submonolayer or minimizing the active species to atoms, the chemical information on interfaces was enlarged. At the atomic scale, the coordination chemistry between metal and the supports changes the electronic state and the binding structure of active sites, and eventually the reaction pathway and catalysis performances, enriching our understanding on the complicated interface chemistry involved in heterogeneous catalysis.

## CONCLUSION AND PROSPECTS

What we summarized in this Perspective is the surface coordination chemistry that is linked to the preparation and surface properties of metal nanomaterials. Although many unique physical and chemical properties of nanomaterials appear at the size scale of nanometers, the chemistry at the molecular level (at subnanometer scale) plays important roles in understanding the essential factors that influence the synthesis and properties of nanomaterials. Surface ligands readily promote both catalytic activity and selectivity of metal nanomaterials via steric and electronic effects. Resolving the detailed molecular structures of surface ligands on metal nanoparticles is critical to decode their surface reaction mechanisms. During the past decade, atomically precise metal nanoclusters have been emerging as an ideal system for fully characterizing the coordination structures of surface ligands on metal nanoparticles using molecular approaches. This model system is expected to continuously contribute to the development of surface coordination chemistry of nanomaterials. Besides the development in understanding the coordination chemistry of organic ligands on metal nanomaterials, two unique catalyst structures, inverse structure with metal nanoparticles partially covered by submonolayer support components, and atomically dispersed structure with single metal sites dispersed on supports, has been designed to understand the local coordination chemistry at the interface.

The development of surface coordination chemistry highly relies on the resolution of surface coordination structure on nanomaterials. Considering most characterization techniques are taking samples' average signals, the surface structure information is often overwhelmed by the signals from bulk. Therefore, together with the development of high-resolution surface spectroscopic techniques (e.g., atomic resolution electron energy-loss spectroscopy, tip-enhanced Raman spectroscopy),<sup>103–105</sup> creating model material systems having ultrathin features is still expected to be a powerful alternative strategy to resolve their surface structures based on currently available techniques. These material systems need to share the similar surface coordination structures with realistic metal nanomaterials, but amplify the surface components for structure characterizations. With no doubt, 1D or 2D ultrathin nanostructures, atomically precise metal nanoclusters, and atomically dispersed metal catalysts will be ideal model systems for investigations before the birth of new techniques to directly characterize the molecular surface structure on nanomaterials. Importantly, the combination of these three different model systems should allow the creation of model materials for investigating the surface coordination chemistry in more complicated systems. For instance, depositing premade well-defined nanoclusters of several metal atoms on ultrathin oxide

supports should yield an excellent system for studying both the metal–support interaction and also metal–metal interaction within the cluster. The synthesis of atomically precise metal–metal oxide hybrid nanoclusters will allow the direct resolution of metal–oxide support interaction using X-ray diffraction. By taking the research advances in the synthesis of well-defined nanomaterials, we believe, in the next decades, the extensive collaborations among materials science, spectroscopy, computational chemistry, and catalysis will push forward the continuous development of surface coordination chemistry of metal nanomaterials, helping to achieve the goal to precisely manipulate their surface properties for chemical applications.

## AUTHOR INFORMATION

### Corresponding Authors

\*nfzheng@xmu.edu.cn

\*gfu@xmu.edu.cn

ORCID 

Nanfeng Zheng: 0000-0001-9879-4790

### Notes

The authors declare no competing financial interest.

## ACKNOWLEDGMENTS

We acknowledge the financial support from NNSF of China (21420102001, 21131005, 21333008), and MOST of China (2015CB932303). We also thank the XAFS station (BL14W1) of the Shanghai Synchrotron Radiation Facility (SSRF). P.X. Liu thanks the support from the National postdoctoral program for innovative talents (BX201600093).

## REFERENCES

- (1) Boisselier, E.; Astruc, D. *Chem. Soc. Rev.* **2009**, *38*, 1759.
- (2) Bell, A. T. *Science* **2003**, *299*, 1688.
- (3) Schaefer, H. E. *Nanoscience: The Science of the Small in Physics, Engineering, Chemistry, Biology and Medicine*; Springer: Heidelberg, 2010.
- (4) Alivisatos, A. P. *Science* **1996**, *271*, 933.
- (5) Zherebetsky, D.; Scheele, M.; Zhang, Y.; Bronstein, N.; Thompson, C.; Britt, D.; Salmeron, M.; Alivisatos, P.; Wang, L.-W. *Science* **2014**, *344*, 1380.
- (6) Yang, Y.; Qin, H.; Peng, X. *Nano Lett.* **2016**, *16*, 2127.
- (7) Yang, Y.; Qin, H.; Jiang, M.; Lin, L.; Fu, T.; Dai, X.; Zhang, Z.; Niu, Y.; Cao, H.; Jin, Y.; Zhao, F.; Peng, X. *Nano Lett.* **2016**, *16*, 2133.
- (8) Owen, J. *Science* **2015**, *347*, 615.
- (9) Tao, A. R.; Habas, S.; Yang, P. *Small* **2008**, *4*, 310.
- (10) Xia, Y.; Xiong, Y.; Lim, B.; Skrabalak, S. E. *Angew. Chem., Int. Ed.* **2009**, *48*, 60.
- (11) Chen, M.; Wu, B. H.; Yang, J.; Zheng, N. F. *Adv. Mater.* **2012**, *24*, 862.
- (12) Tsung, C.-K.; Kuhn, J. N.; Huang, W.; Aliaga, C.; Hung, L.-I.; Somorjai, G. A.; Yang, P. *J. Am. Chem. Soc.* **2009**, *131*, 5816.
- (13) Zhou, K.; Li, Y. *Angew. Chem., Int. Ed.* **2012**, *51*, 602.
- (14) Narayanan, R.; El-Sayed, M. A. *J. Phys. Chem. B* **2005**, *109*, 12663.
- (15) Zecchina, A.; Bordiga, S.; Groppo, E. *Selective Nanocatalysts and Nanoscience: Concepts for Heterogeneous and Homogeneous Catalysis*; Wiley-VCH: Weinheim, 2011.
- (16) Noyori, R. *Nat. Chem.* **2009**, *1*, 5.
- (17) Somorjai, G. A.; Rioux, R. M. *Catal. Today* **2005**, *100*, 201.
- (18) Wu, B. H.; Zheng, N. F. *Nano Today* **2013**, *8*, 168.
- (19) Marvell, E. N.; Li, T. *Synthesis* **1973**, *1973*, 457.
- (20) Schoenbaum, C. A.; Schwartz, D. K.; Medlin, J. W. *Acc. Chem. Res.* **2014**, *47*, 1438.
- (21) Zhao, Y.; Fu, G.; Zheng, N. F. *Catal. Today* **2017**, *279*, 36.
- (22) Huang, W.; Hua, Q.; Cao, T. *Catal. Lett.* **2014**, *144*, 1355.



- (23) Chen, G. X.; Xu, C. F.; Huang, X. Q.; Ye, J. Y.; Gu, L.; Li, G.; Tang, Z. C.; Wu, B. H.; Yang, H. Y.; Zhao, Z. P.; Zhou, Z. Y.; Fu, G.; Zheng, N. F. *Nat. Mater.* **2016**, *15*, 564.
- (24) Xia, Y.; Xia, X.; Peng, H.-C. *J. Am. Chem. Soc.* **2015**, *137*, 7947.
- (25) Peng, Z.; Yang, H. *Nano Today* **2009**, *4*, 143.
- (26) Personick, M. L.; Mirkin, C. A. *J. Am. Chem. Soc.* **2013**, *135*, 18238.
- (27) Lohse, S. E.; Burrows, N. D.; Scarabelli, L.; Liz-Marzan, L. M.; Murphy, C. J. *Chem. Mater.* **2014**, *26*, 34.
- (28) Xiong, Y.; Cai, H.; Wiley, B. J.; Wang, J.; Kim, M. J.; Xia, Y. *J. Am. Chem. Soc.* **2007**, *129*, 3665.
- (29) Huang, X. Q.; Zhang, H. H.; Guo, C.; Zhou, Z. Y.; Zheng, N. F. *Angew. Chem., Int. Ed.* **2009**, *48*, 4808.
- (30) Huang, X. Q.; Zheng, N. F. *J. Am. Chem. Soc.* **2009**, *131*, 4602.
- (31) Zhang, Y.; Grass, M. E.; Kuhn, J. N.; Tao, F.; Habas, S. E.; Huang, W.; Yang, P.; Somorjai, G. A. *J. Am. Chem. Soc.* **2008**, *130*, 5868.
- (32) Carrasquillo, A.; Jeng, J.-J.; Barriga, R. J.; Temesghen, W. F.; Soriaga, M. P. *Inorg. Chim. Acta* **1997**, *255*, 249.
- (33) Huang, X. Q.; Tang, S. H.; Mu, X. L.; Dai, Y.; Chen, G. X.; Zhou, Z. Y.; Ruan, F. X.; Yang, Z. L.; Zheng, N. F. *Nat. Nanotechnol.* **2011**, *6*, 28.
- (34) Ishi, S.; Ohno, Y.; Viswanathan, B. *Surf. Sci.* **1985**, *161*, 349.
- (35) Rose, M. K.; Mitsui, T.; Dunphy, J.; Borg, A.; Ogletree, D. F.; Salmeron, M.; Sautet, P. *Surf. Sci.* **2002**, *512*, 48.
- (36) Schlotterbeck, U.; Aymonier, C.; Thomann, R.; Hofmeister, H.; Tromp, M.; Richtering, W.; Mecking, S. *Adv. Funct. Mater.* **2004**, *14*, 999.
- (37) Siril, P. F.; Ramos, L.; Beaunier, P.; Archirel, P.; Etcheberry, A.; Remita, H. *Chem. Mater.* **2009**, *21*, 5170.
- (38) Li, H.; Chen, G. X.; Yang, H. Y.; Wang, X. L.; Liang, J. H.; Liu, P. X.; Chen, M.; Zheng, N. F. *Angew. Chem., Int. Ed.* **2013**, *52*, 8368.
- (39) Hu, C. Y.; Lin, K. Q.; Wang, X. L.; Liu, S. J.; Yi, J.; Tian, Y.; Wu, B. H.; Chen, G. X.; Yang, H. Y.; Dai, Y.; Li, H.; Zheng, N. F. *J. Am. Chem. Soc.* **2014**, *136*, 12856.
- (40) Chen, M.; Tang, S. H.; Guo, Z. D.; Wang, X. Y.; Mo, S. G.; Huang, X. Q.; Liu, G.; Zheng, N. F. *Adv. Mater.* **2014**, *26*, 8210.
- (41) Tang, S. H.; Chen, M.; Zheng, N. F. *Small* **2014**, *10*, 3139.
- (42) Tang, S. H.; Chen, M.; Zheng, N. F. *Nano Res.* **2015**, *8*, 165.
- (43) Pan, Y.-T.; Yin, X.; Kwok, K. S.; Yang, H. *Nano Lett.* **2014**, *14*, 5953.
- (44) Yin, X.; Liu, X.; Pan, Y.-T.; Walsh, K. A.; Yang, H. *Nano Lett.* **2014**, *14*, 7188.
- (45) Dai, Y.; Mu, X. L.; Tan, Y. M.; Lin, K. Q.; Yang, Z. L.; Zheng, N. F.; Fu, G. *J. Am. Chem. Soc.* **2012**, *134*, 7073.
- (46) Zhao, L.; Xu, C. F.; Su, H. F.; Liang, J. H.; Lin, S. C.; Gu, L.; Wang, X. L.; Chen, M.; Zheng, N. F. *Adv. Sci.* **2015**, *2*, 201500100.
- (47) Wu, B. H.; Zheng, N. F.; Fu, G. *Chem. Commun.* **2011**, *47*, 1039.
- (48) Kang, Y.; Ye, X.; Murray, C. B. *Angew. Chem., Int. Ed.* **2010**, *49*, 6156.
- (49) Wang, C.; Daimon, H.; Lee, Y.; Kim, J.; Sun, S. *J. Am. Chem. Soc.* **2007**, *129*, 6974.
- (50) Lim, S. I.; Ojea-Jiménez, I.; Varon, M.; Casals, E.; Arbiol, J.; Puntes, V. *Nano Lett.* **2010**, *10*, 964.
- (51) Zhang, J.; Fang, J. *J. Am. Chem. Soc.* **2009**, *131*, 18543.
- (52) Chen, G. X.; Tan, Y. M.; Wu, B. H.; Fu, G.; Zheng, N. F. *Chem. Commun.* **2012**, *48*, 2758.
- (53) Wu, J.; Gross, A.; Yang, H. *Nano Lett.* **2011**, *11*, 798.
- (54) Habas, S. E.; Lee, H.; Radmilovic, V.; Somorjai, G. A.; Yang, P. *Nat. Mater.* **2007**, *6*, 692.
- (55) Huang, X. Q.; Zhao, Z.; Fan, J.; Tan, Y. M.; Zheng, N. F. *J. Am. Chem. Soc.* **2011**, *133*, 4718.
- (56) Bhaduri, S.; Mukesh, D. *Homogeneous Catalysis: Mechanisms and Industrial Applications*; Wiley-Interscience: New York, 2000.
- (57) Schmid, A.; Dordick, J. S.; Hauer, B.; Kiener, A.; Wubbolts, M.; Witholt, B. *Nature* **2001**, *409*, 258.
- (58) Niu, Z.; Li, Y. *Chem. Mater.* **2014**, *26*, 72.
- (59) Dance, I. G. *Polyhedron* **1986**, *5*, 1037.
- (60) Wu, B. H.; Huang, H. Q.; Yang, J.; Zheng, N. F.; Fu, G. *Angew. Chem., Int. Ed.* **2012**, *51*, 3440.
- (61) Blaser, H. U.; Jalett, H. P.; Wiehl, J. *J. Mol. Catal.* **1991**, *68*, 215.
- (62) Bürgi, T.; Baiker, A. *Acc. Chem. Res.* **2004**, *37*, 909.
- (63) Meemken, F.; Hungerbühler, K.; Baiker, A. *Angew. Chem., Int. Ed.* **2014**, *53*, 8640.
- (64) Marshall, S. T.; O'Brien, M.; Oetter, B.; Corpuz, A.; Richards, R. M.; Schwartz, D. K.; Medlin, J. W. *Nat. Mater.* **2010**, *9*, 853.
- (65) Kahsar, K. R.; Schwartz, D. K.; Medlin, J. W. *J. Am. Chem. Soc.* **2014**, *136*, 520.
- (66) Pang, S. H.; Schoenbaum, C. A.; Schwartz, D. K.; Medlin, J. W. *Nat. Commun.* **2013**, *4*, 2448.
- (67) Schrader, I.; Warneke, J.; Backenköhler, J.; Kunz, S. *J. Am. Chem. Soc.* **2015**, *137*, 905.
- (68) Kwon, S. G.; Krylova, G.; Sumer, A.; Schwartz, M. M.; Bunel, E. E.; Marshall, C. L.; Chattopadhyay, S.; Lee, B.; Jelinek, J.; Shevchenko, E. V. *Nano Lett.* **2012**, *12*, 5382.
- (69) Jones, S.; Qu, J.; Tedsree, K.; Gong, X.-Q.; Tsang, S. C. E. *Angew. Chem., Int. Ed.* **2012**, *51*, 11275.
- (70) Luksirikul, P.; Tedsree, K.; Moloney, M. G.; Green, M. L. H.; Tsang, S. C. E. *Angew. Chem., Int. Ed.* **2012**, *51*, 6998.
- (71) Jin, R. *Nanoscale* **2010**, *2*, 343.
- (72) Negishi, Y.; Nobusada, K.; Tsukuda, T. *J. Am. Chem. Soc.* **2005**, *127*, 5261.
- (73) Jadzinsky, P. D.; Calero, G.; Ackerson, C. J.; Bushnell, D. A.; Kornberg, R. D. *Science* **2007**, *318*, 430.
- (74) Zhu, M.; Aikens, C. M.; Hollander, F. J.; Schatz, G. C.; Jin, R. *J. Am. Chem. Soc.* **2008**, *130*, 5883.
- (75) Dass, A.; Theivendran, S.; Nimmala, P. R.; Kumara, C.; Jupally, V. R.; Fortunelli, A.; Sementa, L.; Barcaro, G.; Zuo, X.; Noll, B. C. *J. Am. Chem. Soc.* **2015**, *137*, 4610.
- (76) Zeng, C.; Chen, Y.; Jin, R.; Kirschbaum, K.; Appavoo, K.; Sfeir, M. Y. *Sci. Adv.* **2015**, *1*, e1500045.
- (77) Hakkinen, H. *Nat. Chem.* **2012**, *4*, 443.
- (78) Yang, H. Y.; Wang, Y.; Huang, H. Q.; Gell, L.; Lehtovaara, L.; Malola, S.; Häkkinen, H.; Zheng, N. F. *Nat. Commun.* **2013**, *4*, 2422.
- (79) Desireddy, A.; Conn, B. E.; Guo, J.; Yoon, B.; Barnett, R. N.; Monahan, B. M.; Kirschbaum, K.; Griffith, W. P.; Whetten, R. L.; Landman, U.; Bigioni, T. P. *Nature* **2013**, *501*, 399.
- (80) Yang, H. Y.; Wang, Y.; Chen, X.; Zhao, X. J.; Gu, L.; Huang, H. Q.; Yan, J. Z.; Xu, C. F.; Li, G.; Wu, J. C.; Edwards, A. J.; Dittrich, B.; Tang, Z. C.; Wang, D. D.; Lehtovaara, L.; Häkkinen, H.; Zheng, N. F. *Nat. Commun.* **2016**, *7*, 12809.
- (81) Yang, H. Y.; Yan, J. Z.; Wang, Y.; Su, H. F.; Gell, L.; Zhao, X. J.; Xu, C. F.; Teo, B. K.; Häkkinen, H.; Zheng, N. F. *J. Am. Chem. Soc.* **2017**, *139*, 31.
- (82) Wang, Y.; Su, H. F.; Xu, C. F.; Li, G.; Gell, L.; Lin, S. C.; Tang, Z. C.; Häkkinen, H.; Zheng, N. F. *J. Am. Chem. Soc.* **2015**, *137*, 4324.
- (83) Wang, Y.; Wan, X. K.; Ren, L. T.; Su, H. F.; Li, G.; Malola, S.; Lin, S. C.; Tang, Z. C.; Häkkinen, H.; Teo, B. K.; Wang, Q. M.; Zheng, N. F. *J. Am. Chem. Soc.* **2016**, *138*, 3278.
- (84) Li, W.; Wang, A.; Yang, X.; Huang, Y.; Zhang, T. *Chem. Commun.* **2012**, *48*, 9183.
- (85) Tauster, S. J. *Acc. Chem. Res.* **1987**, *20*, 389.
- (86) Stakheev, A. Y.; Kustov, L. M. *Appl. Catal., A* **1999**, *188*, 3.
- (87) Fu, Q.; Wagner, T. *Surf. Sci. Rep.* **2007**, *62*, 431.
- (88) Breyse, M.; Afanasiev, P.; Geantet, C.; Vrinat, M. *Catal. Today* **2003**, *86*, 5.
- (89) Allard, L. F.; Borisevich, A.; Deng, W.; Si, R.; Flytzani-Stephanopoulos, M.; Overbury, S. H. *J. Electron Microsc.* **2009**, *58*, 199.
- (90) Fu, Q.; Yang, F.; Bao, X. *Acc. Chem. Res.* **2013**, *46*, 1692.
- (91) Fu, Q.; Li, W.-X.; Yao, Y.; Liu, H.; Su, H.-Y.; Ma, D.; Gu, X.-K.; Chen, L.; Wang, Z.; Zhang, H.; Wang, B.; Bao, X. *Science* **2010**, *328*, 1141.
- (92) Chen, G. X.; Zhao, Y.; Fu, G.; Duchesne, P. N.; Gu, L.; Zheng, Y. P.; Weng, X. F.; Chen, M. S.; Zhang, P.; Pao, C.-W.; Lee, J.-F.; Zheng, N. F. *Science* **2014**, *344*, 495.

- (93) Rodriguez, J. A.; Liu, P.; Graciani, J.; Senanayake, S. D.; Grinter, D. C.; Stacchiola, D.; Hrbek, J.; Fernandez-Sanz, J. J. *Phys. Chem. Lett.* **2016**, *7*, 2627.
- (94) Flytzani-Stephanopoulos, M.; Gates, B. C. *Annu. Rev. Chem. Biomol. Eng.* **2012**, *3*, 545.
- (95) Yang, X.-F.; Wang, A.; Qiao, B.; Li, J.; Liu, J.; Zhang, T. *Acc. Chem. Res.* **2013**, *46*, 1740.
- (96) Liu, P. X.; Zhao, Y.; Qin, R. X.; Mo, S. G.; Chen, G. X.; Lin, G.; Chevrier, D. M.; Zhang, P.; Guo, Q.; Zang, D. D.; Wu, B. H.; Fu, G.; Zheng, N. F. *Science* **2016**, *352*, 797.
- (97) Kwak, J. H.; Hu, J.; Mei, D.; Yi, C.-W.; Kim, D. H.; Peden, C. H.; Allard, L. F.; Szanyi, J. *Science* **2009**, *325*, 1670.
- (98) Kyriakou, G.; Boucher, M. B.; Jewell, A. D.; Lewis, E. A.; Lawton, T. J.; Baber, A. E.; Tierney, H. L.; Flytzani-Stephanopoulos, M.; Sykes, E. C. H. *Science* **2012**, *335*, 1209.
- (99) Yan, H.; Cheng, H.; Yi, H.; Lin, Y.; Yao, T.; Wang, C.; Li, J.; Wei, S.; Lu, J. *J. Am. Chem. Soc.* **2015**, *137*, 10484.
- (100) Vilé, G.; Albani, D.; Nachtegaal, M.; Chen, Z.; Dontsova, D.; Antonietti, M.; López, N.; Pérez-Ramírez, J. *Angew. Chem., Int. Ed.* **2015**, *54*, 11265.
- (101) Qiao, B.; Wang, A.; Yang, X.; Allard, L. F.; Jiang, Z.; Cui, Y.; Liu, J.; Li, J.; Zhang, T. *Nat. Chem.* **2011**, *3*, 634.
- (102) Yamada, Y.; Tsung, C.-K.; Huang, W.; Huo, Z.; Habas, S. E.; Soejima, T.; Aliaga, C. E.; Somorjai, G. A.; Yang, P. *Nat. Chem.* **2011**, *3*, 372.
- (103) Sun, K.; Liu, J.; Nag, N.; Browning, N. D. *Catal. Lett.* **2002**, *84*, 193.
- (104) Zaleski, S.; Wilson, A. J.; Mattei, M.; Chen, X.; Goubert, G.; Cardinal, M. F.; Willets, K. A.; Van Duyne, R. P. *Acc. Chem. Res.* **2016**, *49*, 2023.
- (105) Zhong, J.-H.; Jin, X.; Meng, L.; Wang, X.; Su, H.-S.; Yang, Z.-L.; Williams, C. T.; Ren, B. *Nat. Nanotechnol.* **2016**, DOI: [10.1038/nnano.2016.241](https://doi.org/10.1038/nnano.2016.241).